BUTTERWORTH HEINEMANN

Polymer Vol. 36 No. 14, pp. 2709–2716, 1995

0032-3861/95/$10.00+0.00

Properties and morphologies of poly(L-lactide): 1. Annealing condition effects on properties and morphologies of poly(L-lactide)

Hideto Tsuji
Technology Development Center, Toyohashi University of Technology, 1-1 Tempaku-cho, Toyohashi, Aichi 441, Japan

and Yoshito Ikada*
Research Center for Biomedical Engineering, Kyoto University, 53 Kawahara-cho, Shogoin, Sakyo-ku, Kyoto 606, Japan
(Received 4 November 1994; revised 7 December 1994)

The effects of annealing on the thermal properties, morphologies and mechanical properties of poly(L-lactide) (PLLA) films were investigated by differential scanning calorimetry, polarizing microscopy and tensile testing. PLLA films prepared by solution casting were annealed by three different processes: process A, direct annealing of the as-cast film; process B, melting and annealing; and process C, melting, quenching and annealing. In the case of process B, the morphology depended strongly on the annealing temperature, while it depended only slightly on the annealing temperature in the case of processes A and C. In process C, nucleation occurred upon quenching or in the process of temperature rise after quenching, and its nucleation density was higher than that obtained by process B. Therefore, in process C, overall crystallization lasted for a shorter time than in process B, and the radius of the spherulites formed was much smaller compared with that of the spherulites formed by process B. The crystallinity and melting temperature increased with increasing annealing temperature and time of processes B and C, whereas in process A the annealing conditions only slightly affected those values. Young's modulus increased with increasing crystallinity for all the films annealed by the three processes. Tensile strength showed similar behaviour to Young's modulus, but decreased when large crystallites or spherulites were formed. In the case of processes A and B, elongation at break decreased with increasing crystallinity.

(Keywords: poly(L-lactide); morphology; properties)

INTRODUCTION

During the past decade poly(L-lactide) (PLLA) has been attracting increasing attention, as it is resorbable in the human body, has high mechanical strength and is non-toxic after biodegradation. Indeed, a large number of investigations have been published on the degradation of this polymer both *in vitro*[1–16] and *in vivo*[4,5,7,16–23]. However, it seems that the accumulation of more data is required to draw generalized conclusions on the biodegradation behaviour of PLLA, as the results reported by many research groups on the biodegradation of PLLA are a little different from researcher to researcher. This may be primarily due to differences in the solid structure and properties of the PLLA specimens that have been used for the degradation study, even if the starting PLLA specimens have similar chemical structures and molecular weights. It is well known that the solid structure of a crystalline polymer like PLLA is greatly dependent on the thermal history and pretreatment it has received[24].

The final objective of our series of studies on PLLA is to elucidate the biodegradation mechanism of PLLA. In this first report we aim at understanding the relationships between the solid structure of PLLA and the annealing conditions. A deep understanding will be required to prepare different kinds of PLLA specimens for the biodegradation study. We start with a single PLLA specimen with a fixed molecular weight and subject it to three different thermal treatment processes. The present study will help us to obtain PLLA specimens having different structures with respect to the crystallinity, crystalline size and spherulite morphology.

EXPERIMENTAL

PLLA was synthesized by the method previously reported[25]. L-Lactic acid with an optical purity of 98% was purchased as 90 wt% aqueous solution from CCA Biochem BV, The Netherlands. The oligomeric PLLA prepared by condensation polymerization of the free acid

* To whom correspondence should be addressed

Table 1 Polymerization conditions and characteristics of PLLA

Polymerization conditions	
Stannous octoate	0.03 wt%
Temperature	140°C
Time	10 h
Characteristics	
$[\eta]$	6.63 dl g^{-1}
M_v	3.9×10^5 g mol^{-1}
M_n(g.p.c)	6.1×10^5 g mol^{-1}
M_w(g.p.c.)	1.33×10^6 g mol^{-1}
M_w/M_n	2.2
$[\alpha]_D^{25}$	−157°

was thermally decomposed to yield the lactide monomer. Ring-opening polymerization was performed for L-lactide in bulk at 140°C for 600 min using stannous octoate (0.03 wt%) as polymerization catalyst[4]. The resulting polymer was purified by reprecipitation using methylene chloride as solvent and methanol as precipitant.

The viscosity-average molecular weight ($\bar{M}_v$) of the polymer was determined from the intrinsic viscosity $[\eta]$ in chloroform at 25°C using the equation[26]:

$$[\eta] = 5.45 \times 10^{-4} \bar{M}_v^{0.73} \quad (1)$$

The specific optical rotation $[\alpha]$ of the polymer was measured in chloroform at a concentration of 1 g dl^{-1} and 25°C using a Perkin-Elmer Polarimeter 241 at a wavelength of 589 nm. The characteristics of the polymer used in this work are listed in *Table 1*, together with the polymerization conditions. The $[\alpha]_D^{25}$ value was approximately −150°, in good agreement with the literature value[27].

PLLA film to be used for the annealing experiment was obtained via the casting method. Methylene chloride solution of PLLA with a polymer concentration of 1.0 g dl^{-1} was cast onto a flat glass plate, followed by solvent evaporation at room temperature for approximately one day. To avoid formation of a highly ordered structure, solvent evaporation was performed more rapidly than in our previous papers (one week)[28–30]. The solvent trapped in the resulting film was extracted with methanol and dried *in vacuo* for a week. A film with a thickness of about 50 μm was used for the mechanical and thermal measurements and one of 25 μm for the morphology study.

Annealing of PLLA films was performed under three different conditions as follows. The as-cast film was placed between two micro-coverglasses of 32 × 18 mm^2 and then sealed in a test tube under reduced pressure. In process A the sealed tube was immersed in an oil bath kept at different annealing temperatures (T_a) ranging from 100 to 160°C for predetermined periods of time (t_a). In process B the sealed tube was first put in an oil bath kept at 200°C for 3 min to melt the polymer and then immersed in an oil bath kept at different T_a for predetermined t_a. In process C the sealed tube was kept at 200°C for 3 min in an oil bath to melt the polymer, followed by quick quenching to 0°C and then immersed in an oil bath for annealing at different T_a for predetermined t_a. All the films were quenched at 0°C after annealing to stop further crystallization. The PLLA films obtained by annealing through processes A, B and C are named films A, B and C, respectively. The appearance of the as-cast and annealed films was opaque except that the melt-quenched film and the film B annealed at 140°C for t_a below 10 min appeared transparent.

The crystallization and melting temperatures (T_c and T_m, respectively) and the enthalpy of crystallization and fusion (ΔH_c and ΔH_m, respectively) were determined for the annealed films with a Shimadzu DT-50 differential scanning calorimeter. They were heated under a nitrogen gas flow at a rate of 10°C min^{-1}. The values T_c, T_m, ΔH_c and ΔH_m were calibrated using indium as standard. The crystallinity (x_c) of the PLLA films was evaluated according to the following equation:

$$x_c(\%) = 100 \times (\Delta H_m + \Delta H_c)/93 \quad (2)$$

where 93 (J/g of polymer) is the enthalpy of fusion of PLLA crystals having infinite crystal thickness reported by Fischer *et al.*[1].

The morphology of the films was studied with a Zeiss polarizing microscope. The films of 25 μm thickness

Table 2 Thermal and mechanical properties of film A annealed at different T_a for different t_a

T_a (°C)	t_a (min)	T_g (°C)	T_c (°C)	T_m (°C)	x_c[a] (%)	σ_B[b] (kg mm^{-2})	E[c] (kg mm^{-2})	ϵ_B[d] (%)
25	600	59		178	46	5.0	181	85
100	600			178	49	5.7	199	39
120	600			178	51	5.7	185	17
140	600			179	52	5.7	200	10
160	600			180	57	5.9	211	6
140	5			178	47	5.3	173	31
140	10			178	49	5.1	182	30
140	20			178	49	5.4	180	24
140	30			178	47	5.2	190	20
140	60			178	49	5.3	170	23
140	600			179	52	5.7	200	10

[a] Crystallinity: $x_c(\%) = 100 \times (\Delta H_m + \Delta H_c)/93$
[b] Tensile strength
[c] Young's modulus
[d] Elongation at break

exhibited a morphology very similar to those 50 μm thick. Since the photo contrast of 25 μm film was much higher than that of 50 μm film, the photos of 25 μm films alone will be shown here. Mechanical properties of the films were measured at 25°C and 50% relative humidity using a tensile tester at a cross-head speed of 100% min^{-1}. The initial length of the specimen was always kept to 20 mm.

RESULTS

Process A

Process A consists of simple annealing of the as-cast film. The thermal properties of film A estimated from the d.s.c. thermograms are given in *Table 2*, together with the mechanical properties, when annealed at different T_a for different t_a. It is seen that annealing caused a significant increase in x_c, T_m, tensile strength (σ_B) and Young's modulus (E) with increasing T_a and t_a. In contrast to σ_B and E, the elongation at break (ϵ_B) decreased with increasing T_a and t_a.

Figure 1 shows the photomicrographs of film A annealed at 140°C for 600 min, together with that of the as-cast film. As is seen, the morphology of film A is very similar to that of the as-cast film, both having dark round regions, which are probably spherulites. This suggests that the ordered structure has already been formed during the solvent evaporation process.

Process B

This process is similar to conventional annealing from the melt, which is widely applied for the investigation of crystalline polymers. The thermal and mechanical properties of film B are given in *Table 3* for different T_a and t_a. It is evident that T_m, x_c and E increased with increasing T_a and t_a, whereas ϵ_B decreases with increasing T_a and t_a. In addition, σ_B increased with t_a but decreased when T_a was raised above 100°C. There was an induction period of about 30 min for the increase in T_m, x_c, σ_B and E.

Photomicrographs of film B annealed at different T_a for 600 min are given in *Figure 2*. As is seen from *Figure 2*, the radius of spherulites of film B increased dramatically from 10 to 150 μm when T_a was increased from 100 to 160°C. This radius dependence of PLLA spherulites formed from the melt on T_a is in good agreement with the results of Marega *et al.*[31] and our recent report where a low-molecular-weight PLLA was used[32]. The spherulite density (*SD*) evaluated from *Figure 3* was 530, 72 and 11 mm^{-2} for T_a = 120, 140 and 160°C, respectively. We could not evaluate *SD* for T_a = 100°C, because of too many small spherulites with unclear boundaries.

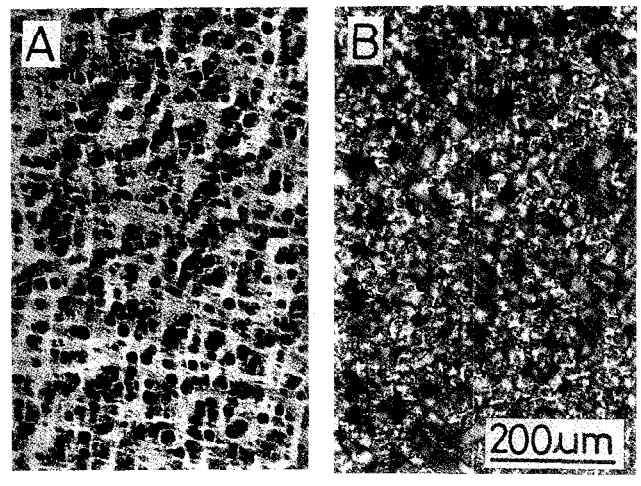

Figure 1 Photomicrographs of: (A) film A (T_a = 140°C, t_a = 600 min); (B) as-cast film

Figure 3 shows photomicrographs of film B annealed at 140°C for different t_a. The spherulites were formed in film B after about t_a = 5 min and then spherulite growth lasted for 60 min. The spherulite radius (r) of film B evaluated from *Figure 3* is plotted as a function of t_a in *Figure 4*. The radial growth rate of the spherulites of film B evaluated from *Figure 3* was 2.0 μm min^{-1} at T_a = 140°C. This value is in agreement with that evaluated by Vasanthakumari and Pennings[33] using the conventional method (2.5 μm min^{-1} for $\bar{M}_v = 3.5 \times 10^5$ and 1.6 μm min^{-1} for $\bar{M}_v = 6.9 \times 10^5$ at 140°C).

Table 3 Thermal and mechanical properties of film B annealed at different T_a for different t_a

T_a (°C)	t_a (min)	T_g (°C)	T_c (°C)	T_m (°C)	x_c[a] (%)	σ_B[b] ($kg\,mm^{-2}$)	E[c] ($kg\,mm^{-2}$)	ϵ_B[d] (%)
0	600	60	114	177	0	5.0	174	27
100	600			177	40	6.2	194	11
120	600			177	47	6.2	190	7
140	600			183	54	5.8	192	6
160	600			191	63	4.5	211	6
140	5	58	108	177	0	4.6	168	22
140	10	58	108	177	0	4.5	172	19
140	20	58	106	177	6	4.6	163	21
140	30	58	108	181	30	5.0	192	18
140	60			182	54	5.6	184	12
140	600			183	54	5.8	192	6

[a] Crystallinity: $x_c(\%) = 100 \times (\Delta H_m + \Delta H_c)/93$
[b] Tensile strength
[c] Young's modulus
[d] Elongation at break

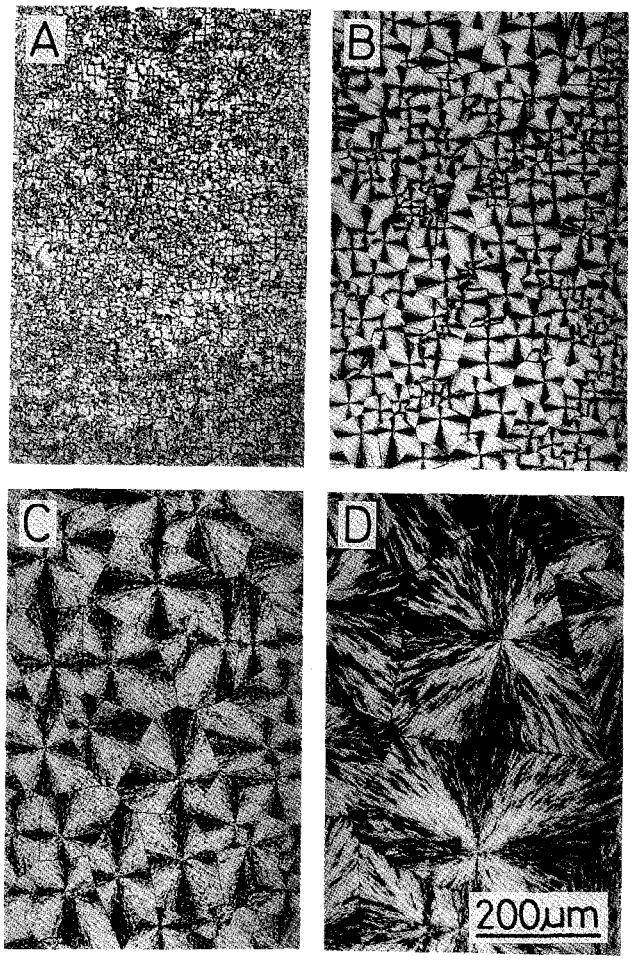

Figure 2 Photomicrographs of film B annealed at different T_a (t_a = 600 min): (A) 100°C; (B) 120°C; (C) 140°C; (D) 160°C

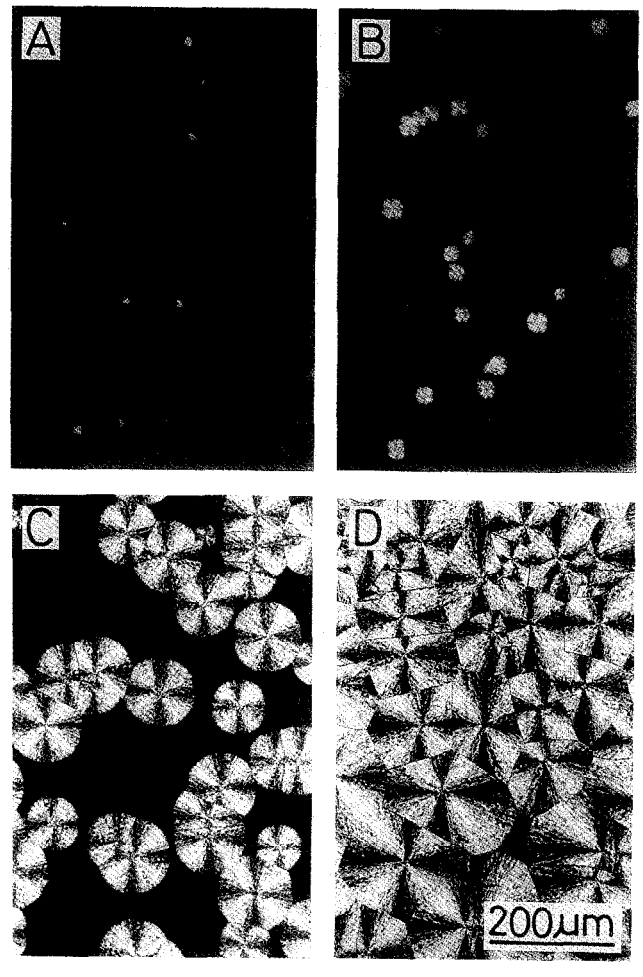

Figure 3 Photomicrographs of film B annealed at different t_a (T_a = 140°C): (A) 5 min; (B) 10 min; (C) 30 min; (D) 60 min

Extrapolation of the spherulite radius to zero in *Figure 4* gives the induction time for spherulite formation. The value was found to be about 3 min. As will be mentioned below, over a half of the film C surface area was covered with spherulites by this time. The apparent induction period for crystallization of film B determined by x_c in *Table 3* (20 min) was longer than that by the spherulite radius in *Figure 4* (3 min).

Process C

Process C involves a quenching process from the melt and subsequent annealing. *Table 4* summarizes the thermal properties of film C estimated from the d.s.c. thermograms for different T_a and t_a, together with the mechanical properties. T_m, x_c and E increased with increasing t_a and T_a, while σ_B increased with t_a but decreased with a rise of T_a. The ϵ_B value of film C did not show any clear dependence on T_a and t_a.

Figure 5 gives photomicrographs of film C annealed at 140°C for different t_a. Comparison between *Figures 3* and *5* reveals that the spherulites in film C were formed more densely than in film B, covering a half of the observation area even by annealing for 3 min. The growing front of the spherulites overlapped each other at about t_a = 5 min, resulting in rapid completion of overall crystallization within 10 min. This is in good agreement with the result reported by Migliaresi *et al.*[34]. The maximum spherulite radius at T_a = 140°C for film C (10 μm) was much smaller than that for film B (120 μm). The morphology of film C

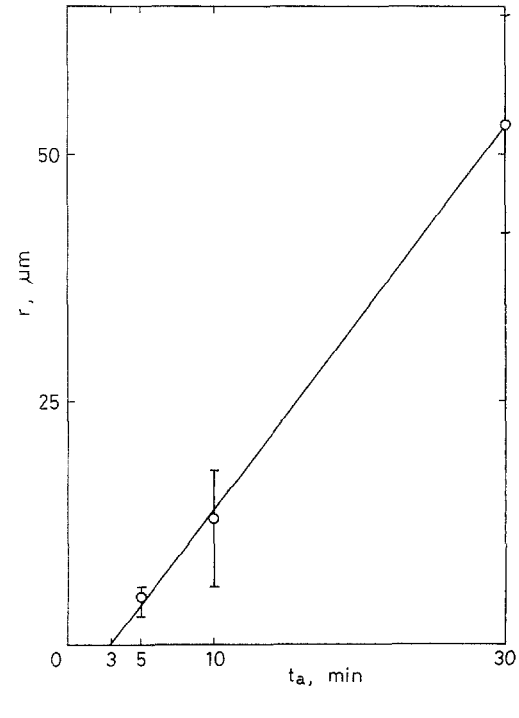

Figure 4 Spherulite radius (r) as a function of time evaluated from *Figure 3*

Table 4 Thermal and mechanical properties of film C annealed at different T_a for different t_a

T_a (°C)	t_a (min)	T_g (°C)	T_c (°C)	T_m (°C)	x_c[a] (%)	σ_B[b] (kg mm^{-2})	E[c] (kg mm^{-2})	ϵ_B[d] (%)
0	600	60	114	177	0	5.0	174	27
100	600			177	39	5.9	178	12
120	600			177	49	5.7	199	5
140	600			182	56	5.6	203	16
160	600			191	65	5.1	216	6
140	3	58	106	177	3	4.9	175	10
140	5	58	103	177	27	5.3	180	12
140	10			180	52	5.7	185	8
140	30			181	54	5.1	185	20
140	60			181	53	5.4	185	10
140	600			182	56	5.6	203	16

[a] Crystallinity: $x_c(\%) = 100 \times (\Delta H_m + \Delta H_c)/93$
[b] Tensile strength
[c] Young's modulus
[d] Elongation at break

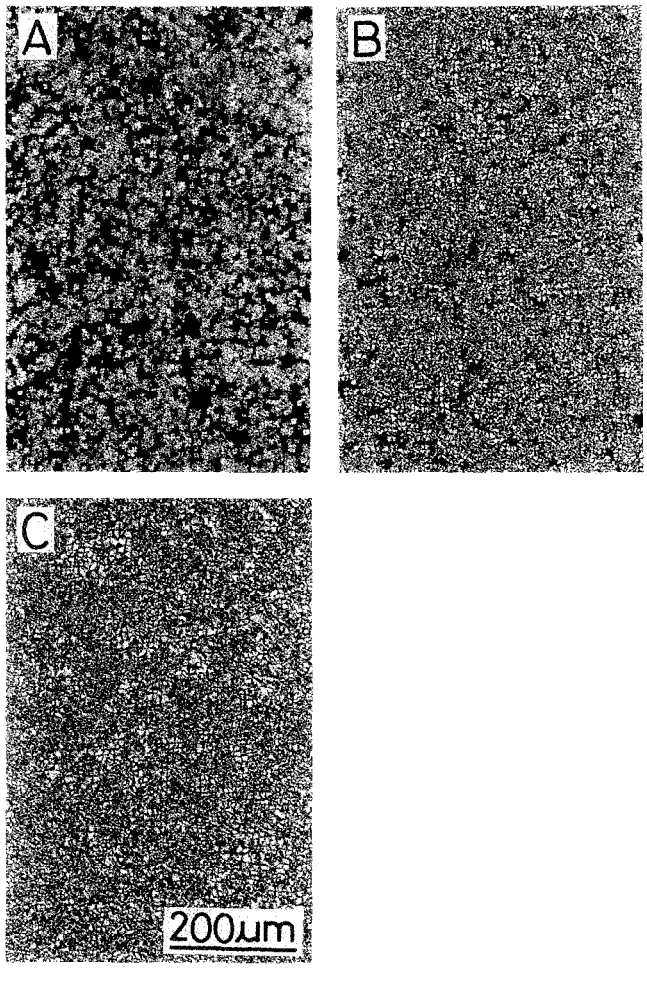

Figure 5 Photomicrographs of film C annealed at different t_a (T_a = 140°C): (A) 3 min; (B) 5 min; (C) 10 min

did not depend practically on T_a at least when annealed at 100 to 160°C for a longer period than 600 min.

Combined process

Combination of two annealing processes by which PLLA films with different morphologies are formed may produce a film having both the morphologies obtained

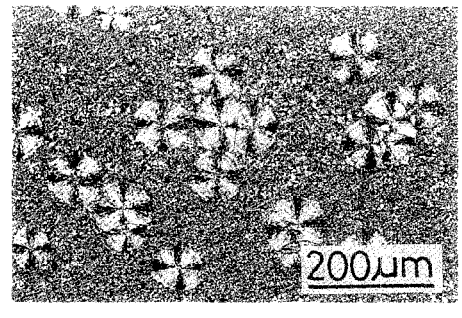

Figure 6 Photomicrograph of PLLA film annealed through the combined process of: melting at 200°C for 3 min/annealing at 140°C for 20 min/quenching at 0°C/annealing at 140°C for 580 min

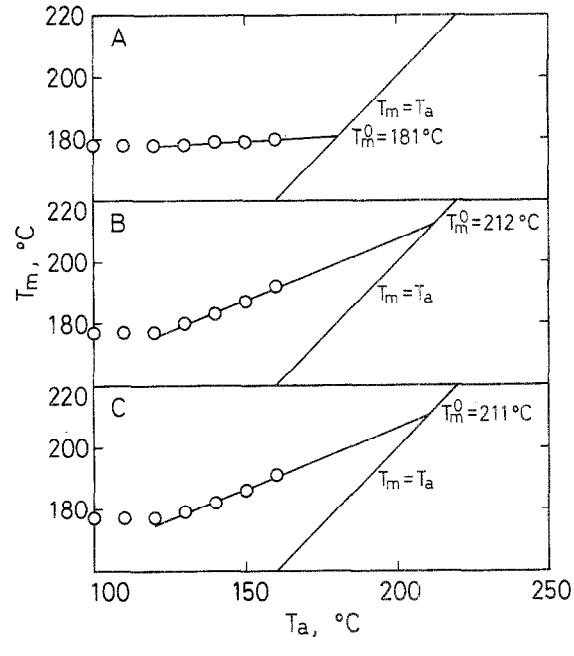

Figure 7 The plots of T_m evaluated from d.s.c. thermograms of PLLA films as functions of T_a (t_a = 600 min): (A) film A; (B) film B; (C) film C

by each of the single annealing processes. *Figure 6* shows one example of a film that was obtained by annealing at 140°C for 20 min after melting (process B), followed by further annealing at 140°C for 580 min after quenching

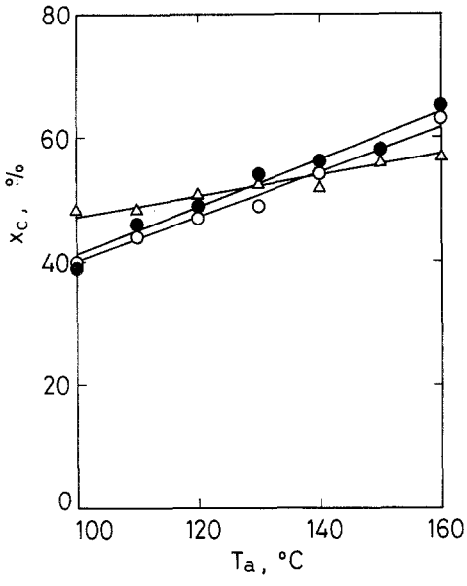

Figure 8 Crystallinity (x_c) evaluated from d.s.c. thermograms of PLLA films as functions of T_a (t_a = 600 min): (△) film A; (○) film B; (●) film C

at 0°C (process C). The values of T_a and total t_a were set to 140°C and 600 min, respectively, similar to that in *Figures 1A* and *2C*. Compared with *Figures 3C* and *5C* it is revealed that this twice-annealed film has the combined morphologies of films B and C annealed at 140°C: that is, relatively large spherulites formed in the first annealing process B, surrounded by many small spherulites formed during the second annealing process C.

Thermal and mechanical properties of films A, B and C

The T_m and x_c values of films A, B and C are plotted as functions of T_a in *Figures 7* and *8*, respectively. Obviously, the dependence of T_m and x_c on T_a is smaller for film A than for films B and C. In addition, x_c and T_m of films B and C increased with the rise of T_a. The equilibrium melting temperatures (T_m^0), estimated by extrapolation of T_m plotted against T_a above 120°C to $T_m = T_a$, were 181, 212 and 211°C for films A, B and C, respectively. Clearly, T_m^0 of film A was much lower than that of films B and C, while T_m^0 of films B and C were very similar to that reported by Kalb and Pennings (215°C)[35].

Values of σ_B and ϵ_B of PLLA films are plotted as a function of T_a in *Figures 9a* and *9b*, respectively. Film B showed the highest σ_B at T_a = 100–140°C, but the lowest at T_a = 160°C among the three films. The σ_B of films B and C decreased at higher T_a, whereas σ_B of film A did not change even if T_a was raised to 160°C. Films B and C did not exhibit a similar dependence of σ_B on T_a, in contrast to that of T_m and x_c, especially at high T_a. The ϵ_B of films A and B decreased with the rise in T_a, finally approaching the same value of 6%. The ϵ_B of film C did not show any definite dependence on T_a.

DISCUSSION

As demonstrated above, the three annealing processes produced PLLA films with different morphological structures and physical properties. The difference between films B and C was not significant but film A had structures and properties fairly different from films B and C. This can be

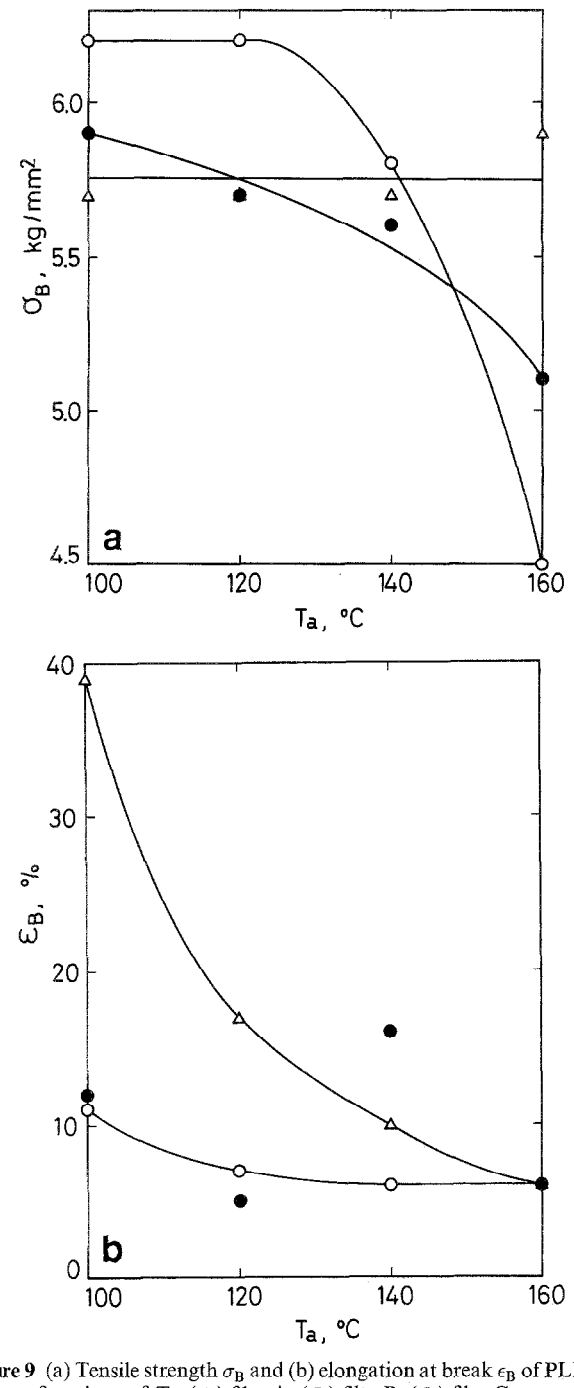

Figure 9 (a) Tensile strength σ_B and (b) elongation at break ϵ_B of PLLA films as functions of T_a: (△) film A; (○) film B; (●) film C

understood in terms of the extent of crystallinity of the PLLA films prior to annealing. The annealing of process A was performed on the as-cast film, which already contained many microcrystallites or spherulites as shown in *Figure 1B* and had a very low potential for additional crystallization by further annealing at higher temperatures. On the contrary, process B started from the annealing of a molten PLLA film without any crystalline region; while the starting film for annealing of process C was also free of crystallites, although the film was in the solid glassy state. Thus, the starting specimens for processes A, B and C were a crystallized film, a molten film and an amorphous film, respectively.

As a result, films B and C showed very similar thermal data (T_m and x_c) (*Figures 7* and *8*) and very similar d.s.c. traces to each other (data not shown) when annealed for

600 min. The average crystal size, crystal-size distribution and crystallinity were very similar between films B and C. On the other hand, the small increase in x_c and T_m observed for film A even at high T_a or long t_a (*Table 2*), in contrast with films B and C, suggests that the network structure linked by the crystallites formed during the solvent evaporation process hindered the recrystallization or formation and growth of crystallites in film A. Equilibrium melting temperature (T_m^0), which is assumed to be the melting temperature of a crystal having infinite size or above which no crystal could exist, was smaller for film A (181°C) than for film B (212°C) and film C (211°C). In the case of film A, the network structure formed during the solvent evaporation process must have hindered the growth of crystals to an equilibrium size and decreased T_m at an arbitrary T_a, resulting in low T_m^0.

The difference between films B and C lies in the spherulite density, which is larger for film C than for film B (*Figures 2C* and *5C*). It is likely that the quenching process before annealing or the process of temperature rise after quenching for process C may have accelerated the nucleation and increased the spherulite density. Higher spherulite nucleation density of film C must have shortened the annealing time required for the completion of overall crystallization and decreased the spherulite radius. As the spherulite nucleation density of film B decreased with a rise of T_a, larger spherulites were formed at higher T_a, in contrast to film C where the spherulite nucleation density or radius seemed to be unchanged by T_a. The independence of the spherulite density or radius of film C on T_a between 100 and 160°C indicates that nucleus formation has almost completed before temperature rise to 100°C. *Figures 7* and *8* imply that one can control T_m and x_c by varying T_a if processes B and C are employed for annealing PLLA. Especially, process C allows us to produce PLLA films with different T_m by varying T_a without the morphology change.

One of the possible reasons for the low σ_B of films B and C at high T_a may be thermal degradation during annealing. However, this is not certain, because σ_B of film A did not change although T_a was raised to 160°C. The finding that T_m of film A was almost independent of T_a and smaller than that of films B and C for all T_a suggests that the crystal size of film A is almost constant and smaller than that of films B and C. These imply that the decrease in σ_B of films B and C at high T_a was due to the formation of large crystallites. The difference in σ_B between films B and C at high T_a may be due to the difference in spherulite radius at high T_a. The spherulite radius of film C was practically constant and smaller than that of film B at T_a = 100–160°C. As mentioned above, the radius of the spherulites of film B increased dramatically with increase in T_a (*Figure 2*), while σ_B decreased. It seems probable that large spherulites may have lowered σ_B of film B at high T_a in good agreement with the literature[24]. All of the E values of PLLA films increased with a rise of T_a and t_a, irrespective of the annealing process. The increase in E must be associated with the increase in x_c of PLLA film resulting from raised T_a and t_a.

It is evident from *Tables 2–4* that σ_B and E of PLLA films increased with increase in x_c, irrespective of T_m or spherulite size. However, there are exceptions. For instance, PLLA films with high T_m (films B and C annealed at 160°C, *Tables 3* and *4*) or large spherulites (film B annealed at 160°C, *Figure 2D* and *Table 3*) have rather low σ_B. As the PLLA films with high T_m may contain large crystallites, large crystallite or spherulite seems to have lowered σ_B, as mentioned above. The spherulite radius itself did not affect the mechanical properties of PLLA films when the radius was below 100 μm. In contrast to E, the ϵ_B of the PLLA films decreased with increase in x_c except for that of film C, which did not show any clear dependence on x_c.

In summary it may be concluded that process B will allow us to obtain various PLLA films having different solid structures and mechanical properties. This is probably because the starting polymer prior to annealing is composed mostly of the amorphous phase, while the other two already contain nuclei and a fraction of crystalline region. The effect of spherulite morphology of PLLA on its degradation in hydrolytic media will be published in the near future.

REFERENCES

1 Fischer, E. W., Sterzel, H. J. and Wegner, G. *Kolloid-Z. Z. Polym.* 1973, **251,** 980
2 Reed, A. M. and Gilding, D. K. *Polymer* 1981, **22,** 494
3 Jamshidi, K. PhD thesis, Kyoto University, 1984
4 Hyon, S.-H., Jamshidi, K. and Ikada, Y. in 'Polymers as Biomaterials' (Eds. S. W. Shalaby, A. S. Hoffman, B. D. Ratner and T. A. Horbett), Plenum Press, New York, 1984, pp. 51–65
5 Jamshidi, K., Hyon, S.-H., Nakamura, T., Ikada, Y., Shimizu, Y. and Teramatsu, T. in 'Biological and Biomechanical Performance of Biomaterials' (Eds. P. Christel, A. Meunier and A. J. C. Lee), Elsevier Science, Amsterdam, 1986, p. 227
6 Pitt, C. G. and Gu, Z. *J. Controlled Release* 1987, **4,** 283
7 Leenslag, J. W., Pennings, A. J., Bos, R. R. M., Rozema, F. R. and Boering, G. *Biomaterials* 1987, **8,** 311
8 Nakamura, T., Hitomi, S., Watanabe, S., Shimizu, Y., Jamshidi, K., Hyon, S.-H. and Ikada, Y. *J. Biomed. Mater. Res.* 1989, **23,** 1115
9 Li, S. M., Garreau, H. and Vert, M. *J. Mater. Sci., Mater. Med.* 1990, **1,** 198
10 Vert, M., Li, S. M. and Garreau, H. *J. Controlled Release* 1991, **16,** 15
11 Matsusue, Y., Yamamuro, T., Oka, M., Shikinami, Y., Hyon, S.-H. and Ikada, Y. *J. Biomed. Mater. Res.* 1992, **26,** 1553
12 Buchholz, B. in 'Degradation Phenomena on Polymeric Materials' (Eds. H. Plank, M. Dauner and M. Renardy), Springer-Verlag, Berlin, 1992, p. 67
13 Dauner, M., Müller, E., Wagner, B. and Plank, H. in 'Degradation Phenomena on Polymeric Materials' (Eds. H. Plank, M. Dauner and M. Renardy), Springer-Verlag, Berlin, 1992, p. 107
14 Verheyen, C. C. P. M., Klein, C. P. A. T., De Blieck-Hogervorst, J. M. A., Wolke, J. G. C., Van Blitterswijn, C. A. and De Groot, K. *J. Biomater. Sci. Mater. Med.* 1993, **4,** 58
15 Migliaresi, C., Fambri, L. and Cohn, D. *J. Biomater. Sci., Polym. Edn.* 1994, **5,** 591
16 Lam, K. H., Nieuwenhuis, P., Molenaar, I., Esselbrugge, H., Feijen, J., Dijkstra, P. J. and Schakenraad, J. M. *J. Mater. Sci., Mater. Med.* 1994, **5,** 181
17 Kulkarni, R. K., Pani, K. C., Neuman, C. and Leonard, F. *Arch. Surg.* 1966, **93,** 839
18 Miller, R. A., Brady, J. M. and Cutright, D. E. *J. Biomed. Mater. Res.* 1977, **11,** 711
19 Vert, M., Christel, P., Chabot, F. and Leray, J. in 'Macromolecular Materials' (Eds. G. W. Hasting and P. Ducheyne), CRC Press, Boca Raton, FL, 1984, p. 119
20 Gerlach, K. L. and Eitenmüller, J. in 'Biomaterials and Clinical Applications' (Eds. A. Pizzoferrato, P. G. Marchetti, A. Ravaglioli and A. J. C. Lee), Elsevier Science, Amsterdam, 1987, p. 439
21 Kaetsu, I., Yoshida, M., Asano, M., Yamanaka, H., Imai, K., Yuasa, H., Mashimo, T., Suzuki, K., Katakai, R. and Oya, M. *J. Controlled Release* 1987, **6,** 249

22 Pistner, H., Bendix, D. R., Mühling, J. and Reuther, J. F. *Biomaterials* 1993, **14,** 291
23 Jadhav, B. S. and Tunc, D. C. in 'Biotechnology and Bioactive Polymers' (Eds. C. Gebelein and C. Carraher), Plenum Press, New York, 1994, p. 169
24 See, for example: Nielsen, L. E. 'Mechanical Properties of Polymers and Composites', Marcel Dekker, New York, Ch. 5
25 Sorensen, W. R. and Campbell, T. W. 'Preparative Methods of Polymer Chemistry', Wiley, New York, 1961
26 Schindler, A. and Harper, D. *J. Polym. Sci., Polym. Chem. Edn.* 1979, **17,** 2593
27 Tonelli, A. E. and Flory, P. J. *Macromolecules* 1969, **2,** 225
28 Tsuji, H., Hyon, S.-H. and Ikada, Y. *Macromolecules* 1991, **24,** 5651
29 Tsuji, H. and Ikada, Y. *Macromolecules* 1992, **25,** 5719
30 Tsuji, H. and Ikada, Y. *J. Appl. Polym. Sci.* 1994, **53,** 1061
31 Marega, C., Marigo, A., Noto, V. D. and Zanetti, R. *Makromol. Chem.* 1992, **193,** 1599
32 Tsuji, H. and Ikada, Y. *Macromolecules* 1993, **26,** 6918
33 Vasanthakumari, R. and Pennings, A. J. *Polymer* 1983, **24,** 175
34 Migliaresi, C., Cohn, D., De Lollis, A. and Fambri, L. *J. Appl. Polym. Sci.* 1991, **43,** 83
35 Kalb, B. and Pennings, A. J. *Polymer* 1980, **21,** 607